

# Surface Properties of the Processing Tool Related to Flow Behavior of PIM Materials

Bc. Vojtěch Palisa

---

Master thesis  
2018



Tomas Bata University in Zlín  
Faculty of Technology

---

Univerzita Tomáše Bati ve Zlíně

Fakulta technologická

Ústav fyziky a mater. inženýrství

akademický rok: 2017/2018

## ZADÁNÍ DIPLOMOVÉ PRÁCE

(PROJEKTU, UMĚLECKÉHO DÍLA, UMĚLECKÉHO VÝKONU)

Jméno a příjmení: **Bc. Vojtěch Palisa**  
Osobní číslo: **T16278**  
Studijní program: **N2808 Chemie a technologie materiálů**  
Studijní obor: **Materiálové inženýrství**  
Forma studia: **prezenční**

Téma práce: **Vliv povrchových vlastností nástroje na tokové chování PIM materiálů**

Zásady pro vypracování:

**The aim of this master thesis is testing of influence of surface properties of processing tool on the flow behavior of highly filled polymer melts employed in powder injection molding (PIM) technology.**

Rozsah diplomové práce:

Rozsah příloh:

Forma zpracování diplomové práce: tištěná

Seznam odborné literatury:

1. R.M. German, Powder Injection Moulding. 1st Ed, Metal Powder Industries Federation, Princeton (1995).
2. HAUSNEROVÁ, B.: Powder Injection Moulding An Alternative Processing Method for Automotive Items. Trends and Developments in Automotive Engineering, Vienna: InTech, p. 129-146 (2011).

Vedoucí diplomové práce: **prof. Ing. Berenika Hausnerová, Ph.D.**  
Ústav výrobního inženýrství

Datum zadání diplomové práce: **2. února 2018**

Termín odevzdání diplomové práce: **18. května 2018**

Ve Zlíně dne 28. února 2018

  
doc. Ing. František Buňka, Ph.D.  
*děkan*



  
doc. Mgr. Aleš Mráček, Ph.D.  
*ředitel ústavu*

## PROHLÁŠENÍ

Prohlašuji, že

- beru na vědomí, že odevzdáním diplomové/bakalářské práce souhlasím se zveřejněním své práce podle zákona č. 111/1998 Sb. o vysokých školách a o změně a doplnění dalších zákonů (zákon o vysokých školách), ve znění pozdějších právních předpisů, bez ohledu na výsledek obhajoby <sup>1)</sup>;
- beru na vědomí, že diplomová/bakalářská práce bude uložena v elektronické podobě v univerzitním informačním systému dostupná k nahlédnutí, že jeden výtisk diplomové/bakalářské práce bude uložen na příslušném ústavu Fakulty technologické UTB ve Zlíně a jeden výtisk bude uložen u vedoucího práce;
- byl/a jsem seznámen/a s tím, že na moji diplomovou/bakalářskou práci se plně vztahuje zákon č. 121/2000 Sb. o právu autorském, o právech souvisejících s právem autorským a o změně některých zákonů (autorský zákon) ve znění pozdějších právních předpisů, zejm. § 35 odst. 3 <sup>2)</sup>;
- beru na vědomí, že podle § 60 <sup>3)</sup> odst. 1 autorského zákona má UTB ve Zlíně právo na uzavření licenční smlouvy o užití školního díla v rozsahu § 12 odst. 4 autorského zákona;
- beru na vědomí, že podle § 60 <sup>3)</sup> odst. 2 a 3 mohu užít své dílo – diplomovou/bakalářskou práci nebo poskytnout licenci k jejímu využití jen s předchozím písemným souhlasem Univerzity Tomáše Bati ve Zlíně, která je oprávněna v takovém případě ode mne požadovat přiměřený příspěvek na úhradu nákladů, které byly Univerzitou Tomáše Bati ve Zlíně na vytvoření díla vynaloženy (až do jejich skutečné výše);
- beru na vědomí, že pokud bylo k vypracování diplomové/bakalářské práce využito softwaru poskytnutého Univerzitou Tomáše Bati ve Zlíně nebo jinými subjekty pouze ke studijním a výzkumným účelům (tedy pouze k nekomerčnímu využití), nelze výsledky diplomové/bakalářské práce využít ke komerčním účelům;
- beru na vědomí, že pokud je výstupem diplomové/bakalářské práce jakýkoliv softwarový produkt, považují se za součást práce rovněž i zdrojové kódy, popř. soubory, ze kterých se projekt skládá. Neodevzdání této součásti může být důvodem k neobhájení práce.

Ve Zlíně .....

.....

---

<sup>1)</sup> zákon č. 111/1998 Sb. o vysokých školách a o změně a doplnění dalších zákonů (zákon o vysokých školách), ve znění pozdějších právních předpisů, § 47 Zveřejňování závěrečných prací:

(1) Vysoká škola nevydělečně zveřejňuje disertační, diplomové, bakalářské a rigorózní práce, u kterých proběhla obhajoba, včetně posudků oponentů a výsledku obhajoby prostřednictvím databáze kvalifikačních prací, kterou spravuje. Způsob zveřejnění stanoví vnitřní předpis vysoké školy.

(2) Disertační, diplomové, bakalářské a rigorózní práce odevzdané uchazečem k obhajobě musí být též nejméně pět pracovních dnů před konáním obhajoby zveřejněny k nahlížení veřejnosti v místě určeném vnitřním předpisem vysoké školy nebo není-li tak určeno, v místě pracoviště vysoké školy, kde se má konat obhajoba práce. Každý si může ze zveřejněné práce pořizovat na své náklady výpisy, opisy nebo rozmnoženiny.

(3) Platí, že odevzdáním práce autor souhlasí se zveřejněním své práce podle tohoto zákona, bez ohledu na výsledek obhajoby.

<sup>2)</sup> zákon č. 121/2000 Sb. o právu autorském, o právech souvisejících s právem autorským a o změně některých zákonů (autorský zákon) ve znění pozdějších právních předpisů, § 35 odst. 3:

(3) Do práva autorského také nezasahuje škola nebo školské či vzdělávací zařízení, užije-li nikoli za účelem přímého nebo nepřímého hospodářského nebo obchodního prospěchu k výuce nebo k vlastní potřebě dílo vytvořené žákem nebo studentem ke splnění školních nebo studijních povinností vyplývajících z jeho právního vztahu ke škole nebo školskému či vzdělávacímu zařízení (školní dílo).

<sup>3)</sup> zákon č. 121/2000 Sb. o právu autorském, o právech souvisejících s právem autorským a o změně některých zákonů (autorský zákon) ve znění pozdějších právních předpisů, § 60 Školní dílo:

(1) Škola nebo školské či vzdělávací zařízení mají za obvyklých podmínek právo na uzavření licenční smlouvy o užití školního díla (§ 35 odst. 3). Odpírá-li autor takového díla udělit svolení bez vážného důvodu, mohou se tyto osoby domáhat nahrazení chybějícího projevu jeho vůle u soudu. Ustanovení § 35 odst. 3 zůstává nedotčeno.

(2) Není-li sjednáno jinak, může autor školního díla své dílo užít či poskytnout jinému licenci, není-li to v rozporu s oprávněnými zájmy školy nebo školského či vzdělávacího zařízení.

(3) Škola nebo školské či vzdělávací zařízení jsou oprávněny požadovat, aby jim autor školního díla z výdělku jím dosaženého v souvislosti s užitím díla či poskytnutím licence podle odstavce 2 přiměřeně přispěl na úhradu nákladů, které na vytvoření díla vynaložily, a to podle okolností až do jejich skutečné výše; přitom se přihlédne k výši výdělku dosaženého školou nebo školským či vzdělávacím zařízením z užití školního díla podle odstavce 1.

## **ABSTRACT**

This diploma thesis deals with the rheological properties of highly filled polymer compounds utilized in powder injection molding (PIM) technology. The main point of this study is the influence of the surface properties and geometry of the extrusion slit die channels on the viscosity and wall slip of the compounds based on aluminum oxide and zirconia oxide powders. The compounds filled close to maximum loading level were prepared by melt mixing, and the obtained samples were then extruded through two slit dies on an on-line rheometer. From the data obtained, the slip velocity was calculated and compared with the roughness of the individual extrusion slit dies. Roughened surface causes decrease in slip velocity.

Keywords: highly filled polymer compound, ceramic powder, slit die, surface roughness, on-line rheometer, wall slip

## **ABSTRAKT**

Tato diplomová práce se zabývá zkoumáním reologických vlastností při zpracování vysoce plněných suspenzních tavenin, které se připravují technologií PIM (Powder Injection Molding). Hlavním bodem studie je vliv povrchových vlastností a geometrie ploché vytlačovací hlavy na tokové chování keramických suspenzí. Testovanými plnivy byly prášek oxidu hlinitého a oxidu zirkoničitého, jež byly zamíchány v koncentracích blízko maximálního plnění pro daný typ materiálu. Získané vzorky byly následně vytlačovány přes speciálně navržené ploché štěrbiny na on-line reometru. Ze získaných dat byla vypočítána skluzová rychlost. Drsnost povrchu snižuje skluzovou rychlost.

Klíčová slova: vysoce plněné polymerní suspenze, keramický prášek, plochá hlava, drsnost povrchu, on line reometr, skluz na stěně

I would like to thank all those people who have been very helpful to me during the measurements and writing of my master thesis, and whose support I really appreciate.

Firstly, I would like to thank my diploma advisor prof. Ing. Berenika Hausnerová Ph.D from Tomas Bata University for her guidance, help and support throughout this research and data evaluation.

Special big thanks belong to Ing. Daniel Sanétník for his assistance with the rheological measurements and also help and support throughout this research and data evaluation and to doc. Dr. Ing. Vladimír Pata for the roughness measurements of slit die channel surfaces

I would also like to thank to the Centre of Polymer Systems TBU in Zlin for providing of selected spaces and measuring equipments.

However, I am of course grateful to my family and close friends for their continuous support during all my studies.

I hereby declare, that this master thesis was carried out independently and only by use of the aids that are stated. I further declare that the presented version of master thesis and the electronic one recorded to IS/STAG are identical.

# CONTENT

<b>INTRODUCTION .....</b>	<b>9</b>
<b>I THEORETICAL PART.....</b>	<b>10</b>
<b>1 ROUGHNESS EVALUATION.....</b>	<b>11</b>
1.1 SURFACE TOPOGRAPHY .....	11
1.2 3D OPTICAL PROFILOMETRY .....	12
1.3 EVALUATION FOR CHARACTERISTIC OF SURFACE IN TURNING .....	13
1.3.1 Quantitative evaluation of machined surfaces .....	13
1.4 SURFACE PARAMETERS .....	15
1.4.1 Arithmetic average height ( $R_a$ ).....	15
1.4.2 Maximum height of peaks ( $R_p$ ) .....	16
1.4.3 Maximum depth of valleys ( $R_v$ ) .....	16
1.4.4 Maximum hight of the profile ( $R_t$ or $R_{max}$ ).....	16
1.4.5 Arithmetic mean deviation of the surface $S_a$ .....	16
<b>2 RHEOLOGICAL DESCRIPTION OF WALL DEPLETION EFACT.....</b>	<b>18</b>
2.1 TRUE SLIP.....	18
2.2 APPARENT SLIP MECHANISM .....	19
2.3 SLIP BEHAVIOR ACCORDING TO DIFFERENT GEOMETRIES .....	20
2.3.1 Tube geometry .....	21
2.3.2 Parallel plates (plane Couette flow) .....	22
2.3.3 Wall slip layer problems .....	23
2.4 PROCESSABILITY .....	24
<b>3 INFLUENCE OF SURFACE ROUGHNESS ON RHEOLOGICAL BEHAVIOR .....</b>	<b>25</b>
3.1 EFFECT OF THE SURFACE ROUGHNESS ON HIGH – FILLED SUSPENSIONS .....	25
3.2 CONSEQUENCE OF $R_A$ ON WALL SLIP .....	26
3.3 INFLUENCE OF DIE ROUGHNESS .....	26
<b>II EXPERIMENTAL PART.....</b>	<b>27</b>
<b>4 FEEDSTOCK CHARACTERISTICS .....</b>	<b>28</b>
4.1 BINDER.....	28
4.2 POWDER.....	28
4.2.1 Aluminum oxide powder.....	28
4.3 ZIRCONIUM OXIDE POWDER.....	29
4.4 FEEDSTOCK MIXING.....	29
<b>5 TESTING METHODS.....</b>	<b>31</b>
5.1 CHANNEL SURFACE MEASUREMENTS .....	31
5.1.1 Surface roughness .....	31
5.1.2 Preparing for measuring surface .....	31



5.2	RHEOLOGICAL MEASUREMENTS .....	32
5.3	ONLINE RHEOMETRY .....	32
<b>6</b>	<b>RESULTS AND DISCUSION .....</b>	<b>34</b>
6.1	SELECTION OF GEOMETRY .....	34
6.2	ROUGHNESS MEASUREMENTS.....	35
6.3	RHEOLOGY .....	36
	<b>CONCLUSION .....</b>	<b>48</b>
	<b>BIBLIOGRAPHY .....</b>	<b>50</b>
	<b>LIST OF ABBREVIATIONS .....</b>	<b>53</b>
	<b>LIST OF FIGURES .....</b>	<b>55</b>
	<b>LISTO OF TABLE .....</b>	<b>57</b>

## INTRODUCTION

For decades, the incorporation of inorganic and organic fillers into a polymer matrix has been of significant industrial importance, as this is one of the most effective ways to develop new materials with enhanced properties for specific applications. The combination of a rigid solid phase and a continuous matrix opens the way to a large field of applications. [1] The rheological behavior of concentrated suspensions has been the subject lot of investigations. Rheology of highly filled suspensions is very important to prerequisite for their ideal processing. Important aspect of the rheological properties of highly filed material applied flow instabilities, shear induced migrations of rigid particles and wall slip. [2]

Grooved or roughened surfaces are often used during the rheological characterization of various materials to eliminate wall slip with different construction materials. Roughened rheometer surfaces are also used during the rheological characterization of materials such as compound of polymeric matrix and powder filler. [3] Wall slip in highly filled suspensions is closely related to migration effects. It is a rheological phenomenon which might cause phase separation during the processing of highly filled suspensions.

An objective of this thesis is to study dependence of surface properties of flow channel on rheological behavior changes of highly filled suspension with the special emphasis on the wall slip phenomenon. The theoretical part describes specifics of surface properties of processing tools, focused on flow channels, and rheological behavior of highly filled suspensions such as occurrence of wall-slip in different geometries and influence of surface roughness on reducing of wall slip. The experimental part includes the study of continuous processing of ceramic compounds with the use of online rheometry.

## **I. THEORETICAL PART**

## 1 ROUGHNESS EVALUATION

Surface roughness is very important for many problems including friction, contact deformation, tightness of contact joints, heat and electric current conduction. Therefore, surface roughness has been the subject of experimental and theoretical research for many decades. The real surface geometry is so complicated that a finite number of parameters cannot provide a whole description. Surface roughness parameters are normally divided into three groups according to its properties and functionality. These groups cover amplitude parameters, spacing parameters and hybrid parameters. Calculations of those parameters is also divided, but into two groups. First one is two dimensional (2D) and second one is three dimensional (3D) analyses. 2D profile analysis has been widely used in science and engineering for more than 50 years. Nowadays, a 3D surface analysis is mostly preferred. 3D roughness parameters are calculated for an area of the surface instead of a single line. Hence, in order to calculate the 3D roughness parameters, the software chooses an area from the surface to be tested and divides it into a number of sections. These sections represent a number of consequent profiles from the surface. On the other hand, the 2D roughness parameters are calculated for each section separately, and the average of each parameter is taken for all sections. [4]

### 1.1 Surface topography

Characterization of surface topography on specific features of mechanical workpieces with complex geometries presents a very important challenge. Such requirements occur across a wide range of products and industries including: medical components, turbine blades, electronics, free form diamond turned parts, injection molding dies, optics, diesel injector nozzles, and many more. Metrology needs for this class of parts are characterized by the desire to scan large areas of the surface located at significant distances from each other on the part in order to properly characterize the quality of the component. In this problem, special machines and tools are needed responding to the requirements of the measurements. Tools such as scanning electron microscopy (SEM) and scanning probe microscopy (SPM) are generally used for measurements on the smaller dimensional scales, but are only capable of scanning small areas and have very limited aspect ratios. These devices are generally

considered as  $2^{1/2}$  D measurement devices, meaning that only portions of the surface can be accessed and characterized. [5]

3-D surface profilometry based on the structured light illumination with advantages of non-contact, non-destructive, quick speed and high accuracy has been increasingly used in many areas such as 3-D sensing, quality control, biomedical engineering, industry monitoring, etc. This technique can be divided into two types according to the structure of measurement. One is the optical 3-D surface profilometry based on trigonometric measurement principle that there exists an angle between the projection optical axis and the observation optical axis. Another is the optical 3-D surface profilometry based on vertical measurement principle that the direction of observation is the same as that of the projection. [6]

## 1.2 3D optical profilometry

Optical components present a number of metrology challenges, including reflectance ranging from mirror like to anti-reflective, slopes from normal to near-vertical, and surface roughness from multi- $\mu\text{m}$  to sub- $\text{\AA}$ . Coherence scanning interferometry (CSI) provides non-contact real topography maps on smooth, high-reflectivity surfaces of less than a nm [7]. High-dynamic-range CSI can measure previously inaccessible high slopes and sub- $\text{\AA}$  roughness, capabilities well-suited for measuring optical components. A modern commercial CSI microscope was used to measure a variety of challenging optical components.[8] The following sections each highlight a different technique to boost dynamic range: dynamic noise reduction (DNR) for detection of weak signals; high dynamic range (HDR) for parts with wide reflectance ranges. Dynamic range can be extended more efficiently for parts having a wide range of reflectance. For a traditional CSI measurement is chosen light level so as to avoid sensor saturation and hence is driven by the highest reflectance in the scene. This doubly penalizes low-reflectance regions, already more prone to data drop-out due to their low contrast interferometric signal, by additionally light-starving them. The HDR approach presented here begins by scanning at a standard non-saturating light level, which presented by the highest-reflectance region in the scene. Results are in next part analyzed to optimize higher light level or levels for follow-on scan or scans catering to lower-reflectance features. The final height map combines the best results all good scans. The process is fully automated and applicable, it is not needed knowledge of reflectance at all or their relative scan location. [8]

### 1.3 Evaluation for characteristic of surface in turning

It is very important that we obtain accurate results that will be relevant to surface treatment properties when testing phase separation on a slit die. This surface treatment must be very precise and comply with clearly defined parameters. Machining is a manufacturing route of flow channels including slit die. The aim of cutting in the context of machining is to produce parts with a specified form and surface characteristics (surface roughness, residual stress, etc.) from a workpiece. In machining, a production engineer needs to determine an extremely large number of cutting conditions, such as tools, cutting oil, cutting speed, feed rate, depth of cut, etc., based on the cutting theory and the expert's experience. Furthermore, when the results of machining do not satisfy the given requirements, the cutting conditions have to be changed and machining needs to be conducted again. The production engineer should use the obtained result along with the cutting theory and their experience in order to investigate why the desired result could not be obtained originally and seek the optimum input conditions. [9]

#### 1.3.1 Quantitative evaluation of machined surfaces

In preparing the surface of the flow channel, we encounter two qualitative/quantitative options for determining roughness during turning. The first is roughness in the cutting direction and the second roughness in the feed direction. Roughness in the feed direction is used to evaluate surface roughness during turning, because it is more important in a number of problems. The following factors influence the roughness in the feed direction:

- Theoretical roughness (roughness determined by the geometry of the tool's cutting edge and the feed rate)
- Tool wear
- Adhesion between the tool and the work piece (built-up edge, etc.)
- Vibration of the cutting system
- Burr of work piece
- Workpiece cracks

However, it is not easy to distinguish the effect of each of these factors on the real surface roughness. Hence, the above mentioned parameters are classified into the following three groups:

- Theoretical roughness
- Roughness due to instability of the machining system (poor precision or vibration due to insufficient rigidity, etc.)
- Roughness due to instability in the cutting process (adhesion or built-up edge, etc.)[9]

## 1.4 Surface parameters

Amplitude parameters are the most important parameters to characterize surface topography. They are used to measure the vertical characteristics of the surface deviations. The following sections give a brief description for each parameter. [4]

### 1.4.1 Arithmetic average height ( $R_a$ )

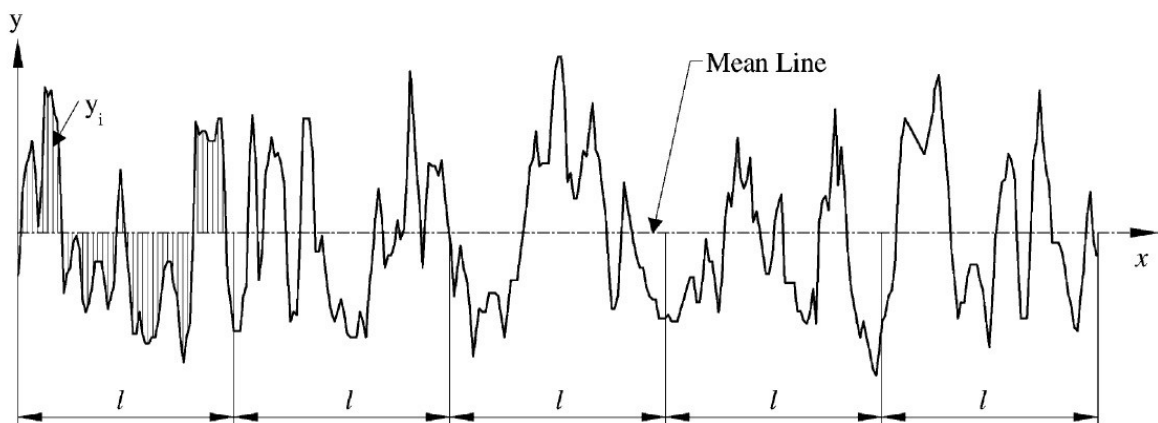


Figure 1 - Definition of the arithmetic average height. [4]

The arithmetic average height parameter ( $R_a$ ), also known as the center line average (CLA), is the most generally used roughness parameter for main quality control. This parameter is easy to define and easy to measure and gives a good general description of height variations of surface. [10] It is defined as the average absolute deviation of the roughness irregularities from the mean line over one sampling length.

This parameter is easy to define, easy to measure, and gives a good general description of height variations. It does not give any information about the wavelength and it is not sensitive to small changes in profile. [4]

It is defined as the average absolute deviation of the roughness changes from the line over one sampling length. The mathematical definition and the digital implementation of  $R_a$  are as follows:

$$R_a = \frac{1}{l} \int_0^l |y(x)| dx \quad (1)$$

where  $l$  is the total length over which the measurements are made.[10]



#### 1.4.2 Maximum height of peaks ( $R_p$ )

$R_p$  is defined as the maximum height of the profile above the mean line within the assessment length as in Fig. 2 In the figure,  $R_{p3}$  represents the  $R_p$  parameter.

#### 1.4.3 Maximum depth of valleys ( $R_v$ )

$R_v$  is defined as the maximum depth of the profile below the mean line within the assessment length as shown in Fig. 2. In the figure  $R_{v4}$  represents the  $R_v$  parameter.

#### 1.4.4 Maximum hight of the profile ( $R_t$ or $R_{max}$ )

This parameter is very sensitive to the high peaks or deep scratches.  $R_{max}$  or  $R_t$  is defined as the vertical distance between the highest peak and the lowest valley along the assessment length of the profile. From Fig. 3:

$$R_{max} = R_p + R_v = R_{p3} + R_{v4} \quad (2)$$

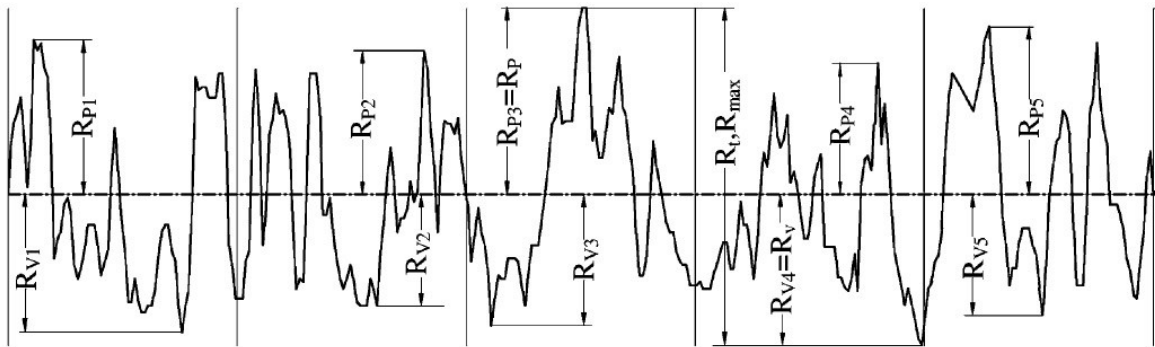


Figure 2 - Definitions of the parameters  $R_v$ ,  $R_p$ ,  $R_t$  ( $R_{max}$ ). [4]

#### 1.4.5 Arithmetic mean deviation of the surface $S_a$

This is a dispersion parameter defined as the arithmetic mean of the absolute values of the surface departures above and below the mean plane within the sampling area ( $R_a$  for 2D). it is given by digital

$$S_a = \frac{1}{MN} \sum_{j=1}^N \sum_{i=1}^M |\eta(x_i, y_j)| \quad (3)$$

$S_a$  is insensitive to the sampling interval but is sensitive to the cut-off if a 2D filter adopted. The 2D counterpart of  $S_a$  is very general and commonly used parameter practical applications.[11]

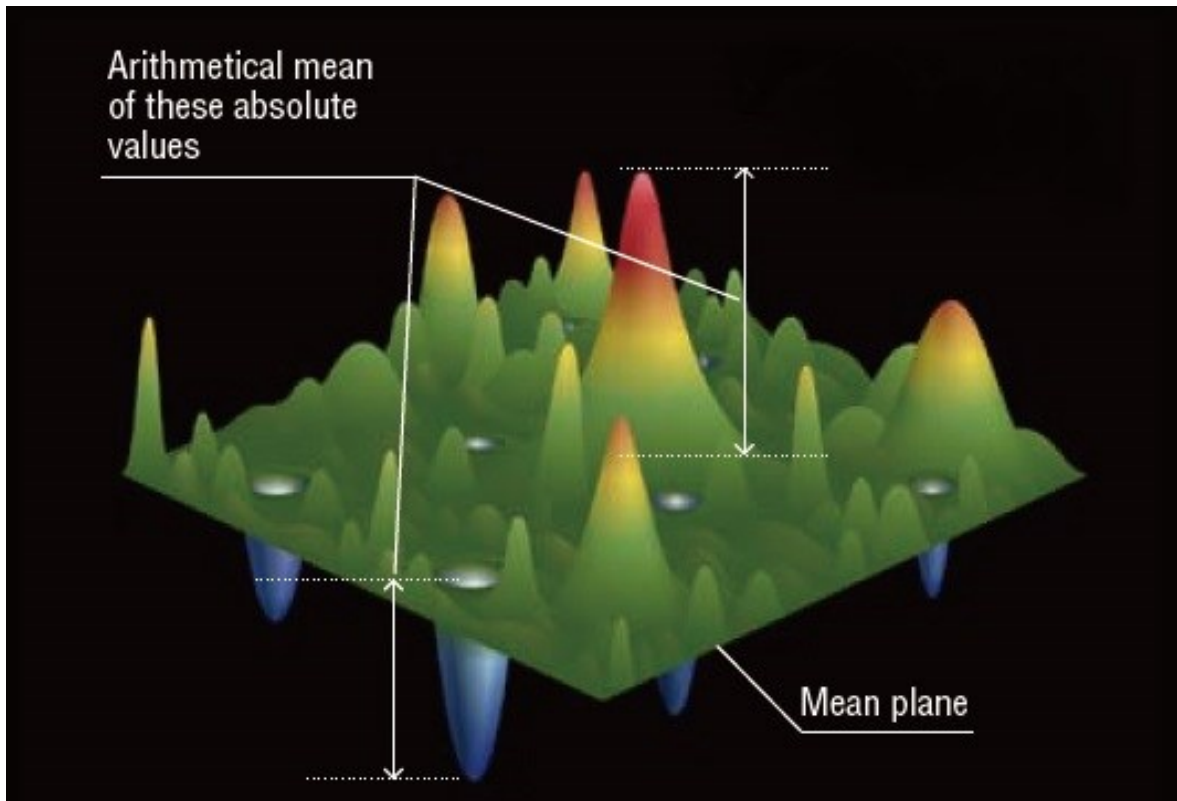


*Figure 3 – Demonstrating of one example evaluation. In actuality, all surface height changes are evaluated[11]*

Surface roughness plays an important role in description of flow behavior of highly filled suspensions. During the flow, it influences the properties of melted liquid inside of exact geometry, and according to the magnitude of roughness, it changes also properties and performance of the final product. The main point of view in this thesis is focused on wall slip effect. It has to be accounted for when investigating phase separation of highly filled compounds, and also it has to be thoroughly investigated.

## 2 RHEOLOGICAL DESCRIPTION OF WALL DEPLETION EFFECT

Slip occurs in the flow of two-phase systems because of the displacement of the disperse phase away from solid boundaries. This arises from steric, hydrodynamic, viscoelastic and chemical forces and constraints acting on the disperse phase immediately adjacent to the walls. The enrichment of the boundary near the wall with the continuous (and usually low-viscosity) phase means that any flow of the fluid over the boundary is easier because of the lubrication effect. [12]

### 2.1 True slip

Slip manifests itself in such a way that viscosity measured in different size geometries gives different answers if calculated in normal way - in particular, the apparent viscosity decreases with decrease in geometry size (e.g. tube radius). Also, in single flow curves, unexpectedly low Newtonian plateaus are sometimes seen, with an apparent yield stress at even lower stresses. Sudden breaks in the flow curves can also be seen. [12] Large (flocculated) particles in a disperse phase, with the large dependence of viscosity on the concentration of the dispersed system are the incentives, which can give slip, if put together with very smooth walls and small flow dimensions. The main liquid materials which give large slip effect on special geometries are concentrated solutions of high molecular weight polymers - for example suspensions of large flocculated particles and emulsions of large droplet sizes.

Until today there are three simple theories of the wall slip effect. The first one assigns wall slip to an adhesive failure of the polymer chains at the solid wall. The second one is a cohesive failure resulting from disentanglement chains between bulk and chains absorbed at the solid wall, thus the polymer is slipping along these absorbed chains. As Fig. 4. presented, this situation is called a true slip .

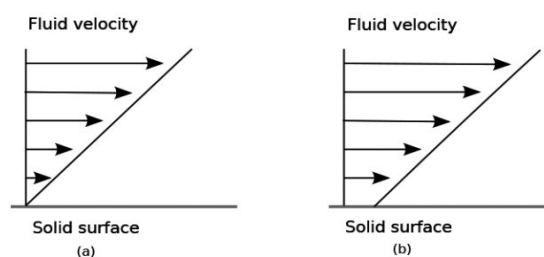


Figure 4 - Differences between no-slip (left) situation and true slip (right). [13]

It emerges from Barnes [9] that when moving the dispersed phase of the material away from the wall, a thin layer with a low viscosity is created at one time and the wall is slipped along its entire length walls due to the lubrication effect. As the concentration of the system increases, the layer becomes thinner and thinner, because the osmotic forces do not have the effect as before. Subsequent enormous increase in bulk viscosity with increasing concentration means that even if thinner, the layer becomes the other side even more important. It is very interesting that very viscous dispersion systems lose their complete adhesion to the walls and slide along them. Acrivos and co-workers [14] have determined the wall-slip velocity values of a concentrated suspension from shear-induced particle migration effects occurring in wide-gapped Couette flow. Allende and Kalyon [15] have demonstrated the effect of wall slip on the migration of particles in the transverse to flow direction in Poiseuille flow. The wall slip of the suspension also affects the filtration based migration of the binder upon jamming of the particles in converging flows Yilmazer.[16]

We can imagine the effects of slipping by taking two or more-phase liquids which are upright with a solid wall, so we can first see physical forces acting. This phenomenon is present even without flow and we should call this the static (no – flow) geometric depletion effect. As well as this, we must also add the extra effect present for very small particles (1  $\mu\text{m}$ ), where the local isotropy of the Brownian motion is destroyed near the walls. When flow works in the bulk fluid, the essential hydrodynamic and entropic forces can move particles off the walls. We can find a lot of special forces, which go against that movement of the particles off the wall. Most interesting and important is osmotic pressure, which arises from concentration gradient. [3]

## 2.2 Apparent slip mechanism

During the flow of a suspension of rigid particles, the particles cannot physically take the space adjacent to a wall as efficiently as they can away from the wall. This leads to the formation of a relatively thin, but always the layer of the fluid adjacent to the wall, the “apparent slip layer” (Fig. 5) or the “Vand layer” [17]. In the beginning of 20<sup>th</sup> century it was detected this layer in his special paint suspension, when flowing under a microscope. Slip comes from a lack of adhesion between wall and flow suspensions [18]. If the dispersion medium consists of a structured fluid, its shear viscosity will vary with structuring parameters. For example, it has been shown that in the case of oleic acid forming the apparent slip layer, the orientation of the oleic acid molecules parallel to the wall reduces "friction,"

i.e., oleic acid acts as a lubricant. On the other hand, when the molecules of oleic acid are oriented normal to the wall, "friction increases", i.e. oleic acid at the wall acts as a "roughening layer". [19]

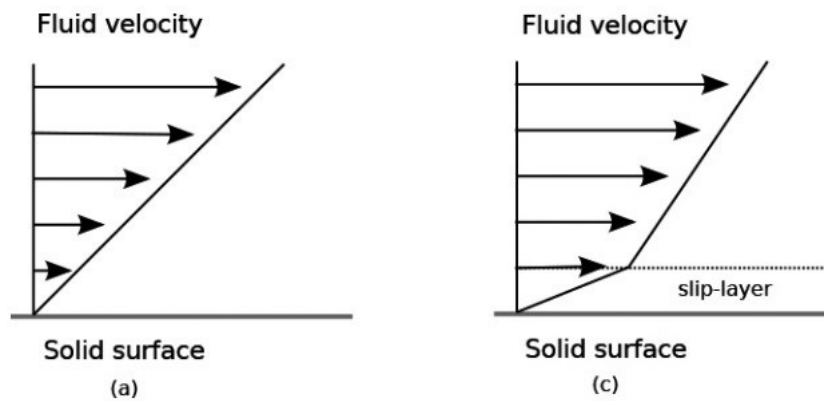


Figure 5 - Differences between no-slip(left) situation and apparent slip(right).[13]

### 2.3 Slip behavior according to different geometries

Wall slip could naturally occurs in all rheometers, because of the presence of the walls. Thus, slip effect exists in geometries such as tubes, cone-and-plate or parallel-plate discs and some other.

Mostly, apparent viscosity calculated increases with a decrease of a certain geometry, e.g. tube radius, gap size, cone angle. In Fig. 6, Mazzanti [20] describes the flow in smooth tubes

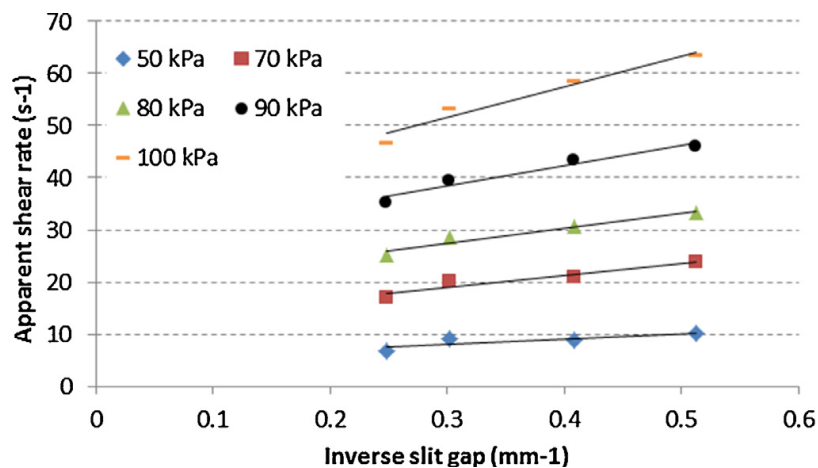


Figure 6 - Wall shear stress vs. apparent shear rate for four slit dies. [20]

of various diameter taken at constant wall shear stress. As it can be seen, the apparent wall shear rate increases as the geometry radius or gap decreases.

An estimate of the slip flow and the bulk flow can be obtained. The main law for slip in a tube says that the shear stress is the same on every single side of borders of a supposed slip layer.

### 2.3.1 Tube geometry

As we can see in Fig. 7, in this geometry, where we assume that there is no moving wall, there is a shear rate profile rising from the center of the flow axis, where its value is the smallest. Furthermore, we can see that the highest melt velocity is at the center of the melt flow, where there will also be the lowest pressure.

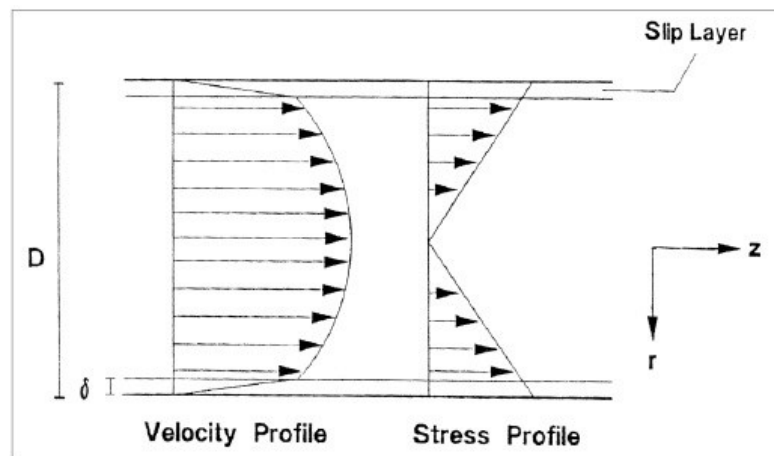


*Figure 7 - Representation of shear stress and velocity profile in capillary flow with apparent wall slip .[21]*

### 2.3.2 Parallel plates (plane Couette flow)

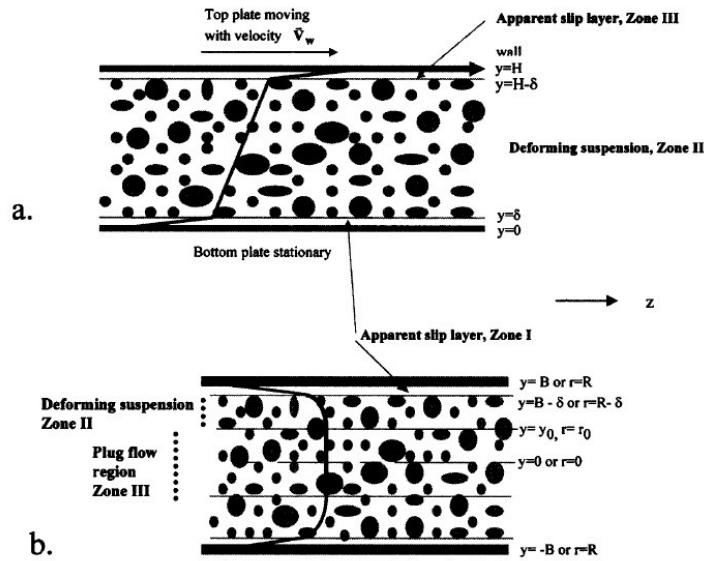


Figure 8 - Schematic representation of the apparent slip flow: (a) in plane Couette (pure drag) flow; (b) in capillary (radius,  $R$ ).[19]

The planar Couette shear flow is the simplest flow that can be generated in the laboratory, typically by means of a sliding plate rheometer. [22] The viscoplastic suspension is flowing under steady-state conditions between two infinitely wide and long plates within a gap of  $H$ , in between two apparent slip layers consisting solely of the binder with thickness  $\delta$  [Fig. 8(a)]. The pressure gradient:

$$\frac{\partial P}{\partial z} = 0 \quad (4)$$

and hence

$$\frac{\partial \tau_{yz}}{\partial y} = 0 \quad (5)$$

For:

$$|\tau_{yz}| \geq \tau_0 \quad (6)$$

the fully developed velocity distributions at the apparent slip layers consisting of the pure binder with thickness  $\delta$ . [18]

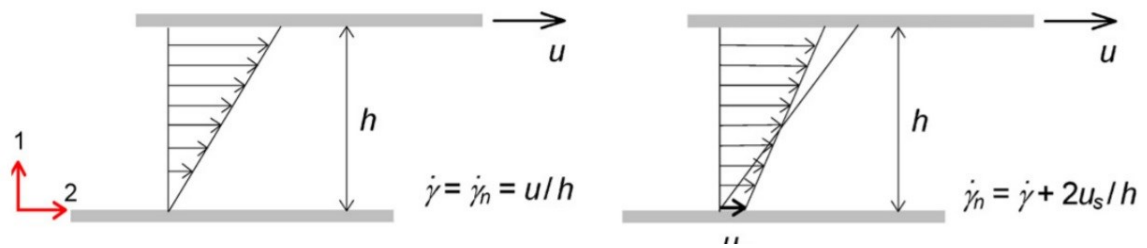


Figure 9 - Velocity profiles in simple shear (plane Couette flow) under no-slip (left) and slip conditions (right).[19]

### 2.3.3 Wall slip layer problems

Fig. 10 illustrates the formation of the apparent slip layer upon the capillary flow of a concentrated suspension of KCl particles (61.9 % by volume and with a mean diameter of 121  $\mu\text{m}$ ) incorporated into an elastomeric binder. Upon exit from the die, the extrudates were fractured and their cross-sections were scanned using SEM and EDX. Fig. 9(a) shows a typical scanning electron micrograph of an extrudate section adjacent to the free surface of the extrudate. The space distribution of the filler particles over the same cross-sectional area was determined using secondary electron microscopic analysis by carrying out elemental mappings of K and Cl elements to identify the KCl particles. Fig. 9(b) shows some of the particles of KCl identified with EDX and the polymeric binder found adjacent to the wall (black zone area). Assuming that the binder at the wall forms the apparent slip layer, the thickness values of this layer were determined to be in the range of 2 to 30  $\mu\text{m}$  (with a mean value of 11  $\mu\text{m}$ , a standard deviation of 6.3  $\mu\text{m}$ ), thus generating a ratio of about 0.09 for the

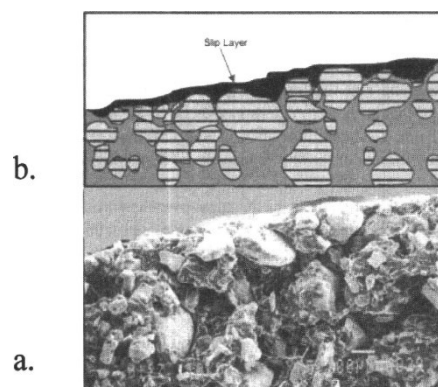


Figure 10 - The formation of the apparent slip layer upon the capillary flow of a concentrated suspension of particles incorporated into an elastomeric binder.[19]



mean thickness of the slip layer over the harmonic mean particle diameter of the rigid particles.

It can come out from Gulmus [3] who studied rheological behavior of concentrated suspension by using parallel disc rheometer. He confirmed that as the solid level increases, the wall slip velocity and the viscosity, corrected for slip effects, also increases. And next very important thing which was obtained, is that as the particle size increases, the wall slip velocity was observed to increase, and the true viscosity was observed to decrease. It is explained by enlarged particles and enlarged space between them. It is important to note that, at low solid levels, the wall slip layer is not significant.

## **2.4 Processability**

The development of the apparent wall-slip layer not only has important consequences for describing of rheological functions of concentrated suspensions, but on their processing and process/product quality control as well. The shape of a slip layer during flow in dies of extruders, and in many of various molding and shaping production routes, changes the processability of suspensions. There are many examples - in single and twin screw extrusions wall slip gets down the pressure rate of the extruder and its distributive and dispersive mixing capabilities. In a die, where suspensions flow, wall slip reduces the pressure drop. [18]

### 3 INFLUENCE OF SURFACE ROUGHNESS ON RHEOLOGICAL BEHAVIOR

#### 3.1 Effect of the Surface Roughness on high – filled suspensions

The rheological behavior of polymeric suspensions governed by the particle shape, size and size distribution, and volume fraction of particles depends also on:

- a) particle – particle interactions
- b) particle – matrix interactions
- c) suspension – processing tool interactions.

Grooved or roughened surfaces are often used during the rheological characterization to eliminate wall slip of various materials. Roughened rheometer surfaces are also used during whole rheological characterization of highly filled suspensions, gels, emulsions, and greases. Using of roughened surfaces eliminates the wall effect, but whole problem depends on a magnitude of roughness. The properties of the wall layer are assessed with the root of the activation energy of the viscous flow of disperse systems. The thickness, concentration of a dispersed phase, and viscosity of the wall layer are determined from the variations of the free activation energy in the wall layer and in the bulk of the fluid. [3]

The flow and deformation behavior of concentrated suspensions is further affected by various structuring phenomena, for example the migrations of particle and matrix, which in process are affected by wall slip. The wall slip of the suspension also affects the filtration based migration of the matrix (binder) upon sink-together of the particles in converging flows. There are many methods for characterization of the wall slip behavior of highly filled suspensions, but it is not only one method, which characterization was the perfect in estimating and predicting that behavior. The development of the apparent slip mechanism upon the formation of a thin slip layer at the wall, consisting only the binder, is used as the basis for solving the velocity distributions of viscoplastic rectangular slit flows. [16], [1], [2]

The flow curves of material should be independent on surface roughness when wall slip does not occur. As it was described in studies by Barnes [12] and Yilmazer [16], slip velocity increases with temperature, and low molecular slip layer increases with increasing size of

the particles. On the other hand Gulmus [3] investigated a significant role of surface roughness to avoid wall slip effect. As shown in Fig. 11, for a die with rough surface solid particles can move into the small holes, and the whole material flow without forming a slip layer.

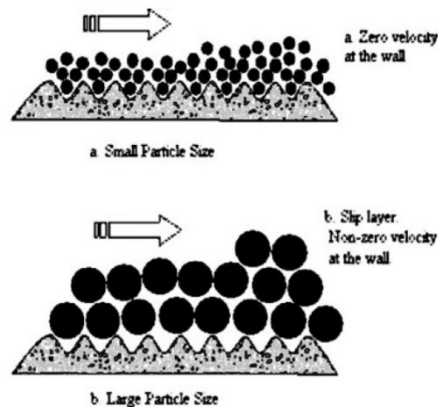


*Figure 11 - Schematic diagram for the effect of  $R_a$  size ratio on the wall slip velocity.[3]*

### 3.2 Consequence of $R_a$ on wall slip

As shown in Fig. 10, when small size particles flow over a surface with roughness comparable to the average particle size, the roughness effects may have prevented slip, and the velocity of the particles near the wall was zero. On the other hand, if the sizes of the particles were much larger than  $R_a$ , the flow of particles was not affected by  $R_a$ , a slip layer formed, and the suspension exhibited slip at the wall. [22]

### 3.3 Influence of die roughness

On three dies with same parameters, but different roughness it has been found that the die with the most roughened surface has the largest pressure drop. Decreasing die wall roughness was also found to reduce flow instabilities seriously. A possible explanation for this is that there is an increase in partial wall slip with decreasing dies surface roughness. Slip at the wall will lower the wall stress, and consequently the extrusion pressure. The reduction of instabilities could be attributed to the delayed separation of the melt from the die, which appeared to occur for decreasing die surface roughness.[3], [1]

## **II. EXPERIMENTAL PART**

## 4 FEEDSTOCK CHARACTERISTICS

Highly filled (powder injection molding) compounds were investigated in this work. They consisted of two types of ceramic powders filled into a thermoplastic binder.

### 4.1 Binder

A polymer binder used in this thesis is composed of 53 % low-density polyethylene, 21 % paraffin wax and 26 % ethylene-vinyl acetate copolymer (Table 1). Relative density of whole binder is  $0.921 \text{ g}\cdot\text{cm}^{-3}$ .

*Table 1 – Characteristic of the binder.*

Binder	Weight [%]	Density [ $\text{g}\cdot\text{cm}^{-3}$ ]
Low-density polyethylene - LDPE	53	0.920 - 0.933
Ethylene-vinyl acetate - EVA	26	0.926 - 0.950
Paraffin wax - PW	21	0.870 – 0.930

### 4.2 Powder

#### 4.2.1 Aluminum oxide powder

$\text{Al}_2\text{O}_3$  powder is a highly compressible superground alumina (Table 1 and Fig. 11) used as a reactive binding component for refractory products as well as for high performance parts.

*Table 2 - Characteristic of aluminum oxide powder.*

Producer	MARTOXID®, MR70
Powder	Aluminum oxide
Density	2.15 – 2.38
Spec. surface area [ $\text{m}^2/\text{kg}$ ]	6 to 10

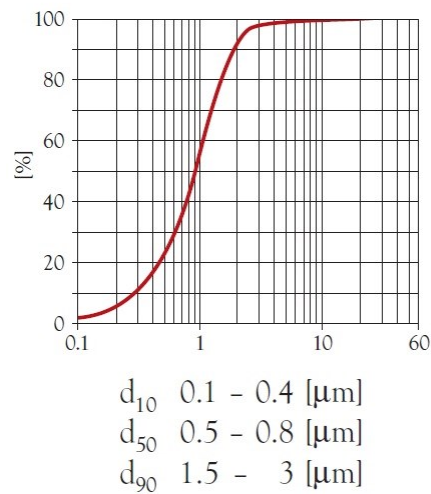


Figure 12 - Particles size distribution of aluminum oxide.

### 4.3 Zirconium oxide powder

Second tested powder was zirconium oxide (Table 3.)

Table 3 - Characteristic of zirconia oxide powder.

Producer	Vibrom
Powder	Zirconium oxide
Density	5.74
Spec. surface area [ $\text{m}^2/\text{kg}$ ]	2.096
Dv (10) [ $\mu\text{m}$ ]	1.69
Dv (50) [ $\mu\text{m}$ ]	3.24
Dv (90) [ $\mu\text{m}$ ]	6.05

### 4.4 Feedstock mixing

As Supati [23] investigated, feedstock preparation for PIM is a crucial step since deficiencies in quality of the feedstock cannot be corrected by subsequent processing adjustments. Hence, it is important that the feedstock is homogeneous and free of particle segregation. Failure to disperse the powder uniformly will cause molding defects such as distortions, cracks, or voids which will lead to non-uniform shrinkage or warping in the sintered parts. The quality

of the feedstock in the mixing process depends on numerous parameters such as mixing time, mixing temperature, powder size, formulation of binder, and powder loading.

Our mixing process was made in Plastometer/Brabender with a twin screws extruder set-up. Temperature set on first zone of screws was 130 °C, in second zone 140 °C and at the end of extruder it was 150 °C. Stable temperature during mixing process is very important to avoid inhomogeneous areas of agglomeration in final product, which may act to broaden the particle size distribution, and reduce the viscosity. To maintenance stable temperature was controlled screw speed because of high dissipation occurrence, which increase the temperature. Size of the riggit particles is other significant parameter which occurs feedstock mixing process. Alumina oxide has smaller riggit particles than zirconia oxide and its mixing process was more difficult to avoid material stack in extrusion/mixing system, because of friction forces. Thus, the screw speed during mixing alumina oxide compound had to smaller than during the mixing zirconia oxide compound. Finally, the compounded material was granulated on a grinding machine, and it was prepared for following rheological measurement.

## 5 TESTING METHODS

### 5.1 Channel surface measurements

#### 5.1.1 Surface roughness

The measurements of surface quality of used flow channels were carried out on the machine ZYGO NEWVIEW, which is intended for non - contact measurements in a workshop environment. The measurement is based on Coherence Scanning Interferometry (CSI) technology, which delivers sub-nanometer precision at all magnifications and measures. Its main advantage is a wide range of surface types, including smooth, rough, flat, sloped, and stepped. All measurements are nondestructive, fast, and require no sample preparation.

#### 5.1.2 Preparing for measuring surface

This profilometer requires exact conditions for the best match measuring. Whole machine stands on four air valve table, witch stabilizes it on horizontal position and prevent vibrations from entire space about. At the beginning of measuring process of slit die, an exact area of a flow channel was chosen, where the lens were focused by a special hand joystick.

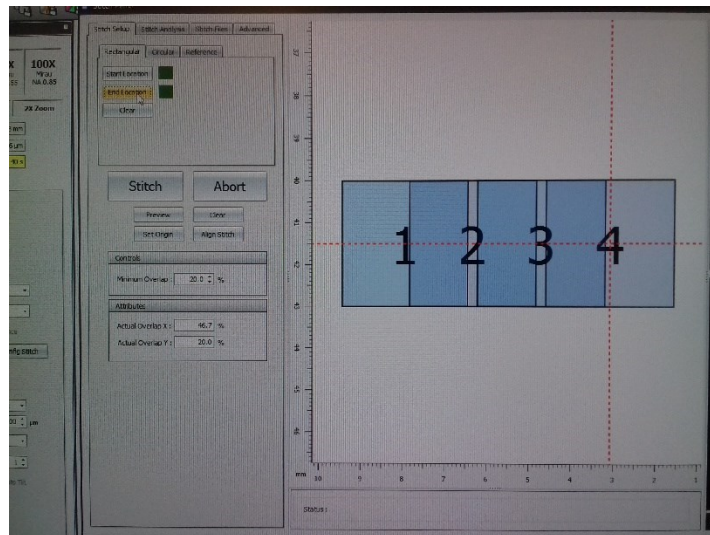
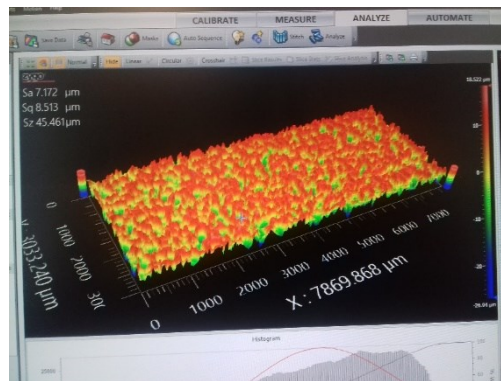


Figure 13 - Setting of three locations of measuring.



After mechanical focusing, there is a software, where an additional information as a type of measuring and scan length was set, and then the most important step was setting of chosen location of flow channel, which was divided into three parts: start, middle, end as shown in Fig. 13. Then, main profile measurement of surface may start. Measured data must be tuned to the required state by using other special software. At the end, exact surface character and roughness parameters were evaluated characterizing flow channel of the die(Fig. 14).



*Figure 14 - The last output of ZYGO software with evaluated parameters and graphically presented surface.*

## 5.2 Rheological measurements

### 5.3 Online rheometry

A slit die rheometry using speeds typical for extrusion process was set as a method suitable for the investigation of wall-slip of PIM materials. The rheological measurements focused on wall-slip were performed on online rheometer (Brabender Extrusiograph 19/25D). The material was first melted under conditions define in the Chapter 4.4, and then extruded through the slit dies with dimensions (10x1x100) mm and (10x2x100) mm. In order to study the impact of pressure conditions on wall-slip effect of the materials the dies were modified by insertion of movable valve enhancing the pressure growth on suspension melt. The valve was alternated in three positions; fully open, half-closed and fully closed. While the complete closure of the valve caused the greatest pressure growth on the polymer melt, in open position the pressure conditions were not increased at all. The dies were equipped with three pressure transducers ( $p1 - p3$ ) in order to evaluate shear viscosity from pressure gradient

inside the flow channel. Transducer  $p_3$  relates to pressure at the entrance to the flow channel and  $p_1$  to pressure at the exit of the flow channel. The scheme of arrangement of pressure transducers is shown in Fig. 16. The temperatures of individual zones (1 – 4) were controlled and displayed by electronic temperature controllers. Measuring value, pressure, was recorded continuously by program Visco and represented in the form of tables and diagrams parallel to the current test.

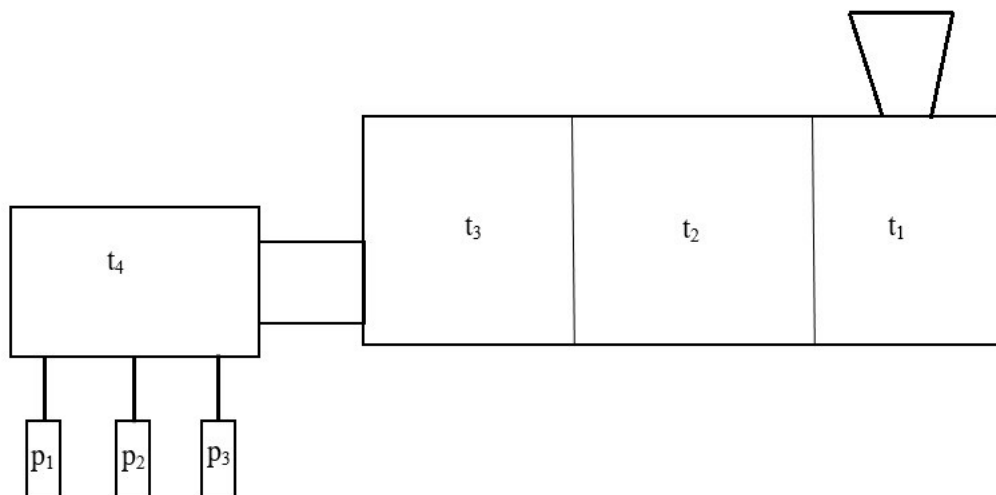


Figure 15 - Scheme of measuring device with representation of pressure ( $p_1 - p_3$ ) and individual temperature zones (1, 2, 3 – extruder; 4 – slit die).

## 6 RESULTS AND DISCUSSION

### 6.1 Selection of geometry

Lots of investigations about measurement device for highly filled suspensions studied the typical rheological behavior during the extrusion in lab, because they are similar to conditions in practice. In the study of Steffe [24], an online rheometry is presented as most accurate way to measure such properties. Slit die rheometry and capillary rheometry are the common used methods to measure the rheological behavior of highly filled suspensions online. The point of that case lies in mounting the geometry on the extruder. Typical geometry and most used for online measurement is slit die, because the mounted pressure transducers allow measuring the pressure directly on the input and on the output of the flow channel without any disturbance of the flow..

Han [25] in his investigation about flow behavior of melted polymers, where used two rectangular dies with different gaps, proposes that rheological properties from slit die rheometry should coincide with capillary rheometer. During the flow of highly filled polymer melts we have to account for the wall slip in both rheometers. Question is, if we need to eliminate wall slip or preserve it. For our purpose to describe behavior of suspensions is the best way characterized the wall slip, because that effect is desirable, thus not to be eliminated. The main point is the incorporation of wall slip behavior into the analysis to indicate and/or eliminate the phase separation of the individual material components. Slit die as an alternative geometry to the parallel plate discs, enhances the wall slip effect, because there is a shear stress gradient present during the flow. However, slip is highly influenced by abrasive properties of melt suspensions. In many papers, the flow properties on the walls of various geometries are described, but without concern on gradual changes of surface of the die depending on a number of extrusion circles.

In this investigation, two types of slit dies were used. As Barnes [3] said in his investigation, different gaps, thought the smaller one, is one of the reasons of the wall depletion effect. Therefore, decisive geometry size was selected, and on the other hand, surface roughness of flowing channel as well. The roughness of the channel surface was adjusted, because even for rheologically simpler materials as pure polymer melts, the surface of the walls plays an important role in determination of the wall slip. The geometries used for measurements were following:

- Slit die with parameters (10/1/100) mm, smooth surface
- Slit die with parameters (10/1/100) mm, roughened surface
- Slit die with parameters (20/1/100) mm, smooth surface
- Slit die with parameters (20/1/100) mm, roughened surface

where the parameter  $H/W/L$  indicates the ratio of the height  $H$  to width  $W$  to length  $L$  of slit die channel.

## 6.2 Roughness measurements

Roughness measurement and surface topography of slit die channels have been done on profilometer ZYGO NEWVIEW, which base on Coherence scanning interferometry (CSI) provides non-contact real topography maps on smooth, high-reflectivity surfaces of less than nm. This device have done all of the geometries what was used for measuring. The channel surfaces were describe by the special 3D roughness parameter  $S_a$ , which is most used parameter for classifying of roughness profile. Meaning of this parameter is seriously described in previous section, in nutshell it is the arithmetical average of the peaks of all profile values from the mean area.

*Table 4 - The roughness parameters of smooth and roughened slit die flow channels.*

Slit die 10/1/100 (mm)					
Smooth surface			Roughened surface		
	$S_a$ ( $\mu\text{m}$ )	$S_z$ ( $\mu\text{m}$ )		$S_a$ ( $\mu\text{m}$ )	$S_z$ ( $\mu\text{m}$ )
start	0.81	6.19	start	9.54	57.35
middle	0.78	5.49	middle	9.91	60.99
end	0.85	6.48	end	9.51	54.40
Slit die 10/2/100 (mm)					
Smooth surface			Roughened surface		
	$S_a$ ( $\mu\text{m}$ )	$S_z$ ( $\mu\text{m}$ )		$S_a$ ( $\mu\text{m}$ )	$S_z$ ( $\mu\text{m}$ )
start	0.80	6.67	start	7.93	49.28
middle	0.88	6.98	middle	6.99	46.76
end	0.77	6.33	end	8.69	59.85

### 6.3 Rheology

In this thesis, the wall slip of ceramic compounds were measured with online rheometer, where screw speed ranged from 5 to 100 rpm. The extruded samples were taken from the extrusion die at intervals which varied according to the screw rotations. Next step of process comprised to weight extruded samples, and then the shear stress  $\tau$  and shear rate  $\dot{\gamma}$  were evaluated

At the beginning, the volumetric flow rate  $\dot{Q}$  (m<sup>3</sup>/min):

$$\dot{Q} = \frac{V}{t} \quad (7)$$

where  $V$  (mm<sup>3</sup>) is the volume of the fluid, which passes through a given surface per unit time  $t$  (s). The shear stress  $\tau$  (Pa) corrected by the use of Bagley-pressure correction is calculated by the measured pressure drop  $\Delta p$  at a certain volumetric flow rate  $\dot{Q}$ :

$$\tau = \frac{(p_3 - p_1) \cdot H}{2L} \quad (8)$$

where  $p_3$  (Pa) is the pressure value on the start of the flow channel,  $p_1$  (Pa) is the pressure on the finish of the channel,  $H$  (mm) describe the height of the slit die and  $L$  (mm) is the length between pressure transducers  $p_3$  and  $p_1$ . After that step is needed the apparent shear rate  $\dot{\gamma}_a$  (s<sup>-1</sup>):

$$\dot{\gamma}_a = \frac{6 \cdot \dot{Q}}{H^2 \cdot W} \quad (9)$$

where  $W$  (mm) describe the width of slit geometry.

The first feedstock, composed of binder and zirconium oxide powder, was processed at three temperature settings. First setting was: 130 °C, 135 °C, 140 °C, 140 °C, next one was 130 °C, 140 °C, 150 °C, 150 °C, and the last setting: 135 °C, 145 °C, 160 °C, 160 °C. The first three temperatures were set for the extrusion screw, and the last two corresponds to zones at the slit die. The flow curves for (10/1/100) mm and (10/2/100) mm slit were evaluated from the measured data. As it can be seen, surface roughness of flow channel unambiguously affects rheological behavior. Using the rough surface slit die reduces the slipping of the wall and higher values of shear stress are obtained.

First die which was tested on rheological behavior during process had a smooth surface and dimensions were (10/1/100) mm and (10/2/100) mm. In dies with smooth surface, smaller pressure gradient was expected than with the rough surface; therefore, sensors with smaller limit could be used. The first sensor  $p_1$  was situated in the end of die and had magnitude 0 – 100 bar, in the middle was sensor  $p_2$  with magnitude 0 – 350 bar and on the start was the sensor  $p_3$  with magnitude 0 – 500 bar. It was expect that pressure variation will be bigger at lower temperatures. Second die had a roughened surface and geometry shape was the same like below. There have been selected pressure sensors valve with bigger range because of roughness surface. Roughened surface eliminates the wall slip, thus pressure in flow channel rapidly increases, mainly in smaller 1 mm channel. Pressure valve with range 0 – 350 bar was chosen at the end of the die, with the range 0 – 500 bar in the middle and valve with range 0 – 700 was situated at the start of flow channel. In following flow curve figures of roughened die is presented only for 160 °C, because the measurement with lower temperatures (140°C, 150°C) could be not carried out for this type of suspension. It was repeatedly controlled and properly measured; however, the pressure at the first zone of the flow channel was too high that pressure valve showed maximum value of its range (700 bar). For that reason measurement was always stopped at a screw speed of 30 rpm. This problem could be sorted by using the control sensors, which their range of monitoring pressure was applied higher than 700 bar, but at the beginning of our investigation it was not expected higher pressure than 700 bar. Sensors with higher range than 0 - 700 was not available in laboratory.

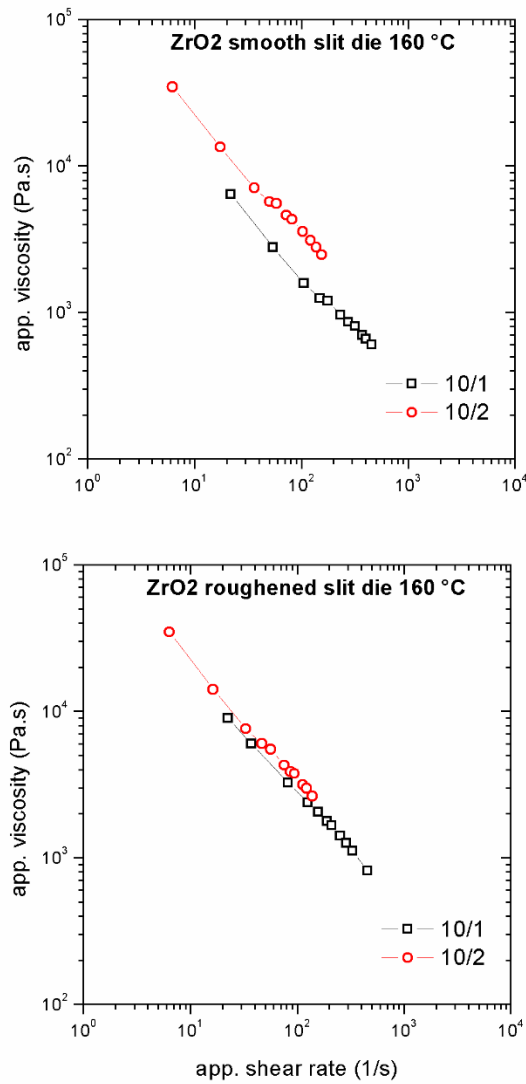


*Figure 16 – App. viscosity as the function of app. shear rate for zirconia oxide compound extruded through smooth and roughened slit die with parameters (10/1/100) mm and (10/2/100) mm. The used temperature (related on die section) was 160°C. Differences between gaps in individual surface roughness.*

Main point of the thesis is based on investigations differences between smooth and roughened surfaces. Fig. 16. presents difference in flow behavior in smooth channel surface, when the gap of channel is 1 mm and 2 mm. On the other side, Fig. 16. also depicted much smaller changes between gaps in situation of roughened flow channel. Nevertheless, the viscosity dependent on geometry shows the slip at the wall.

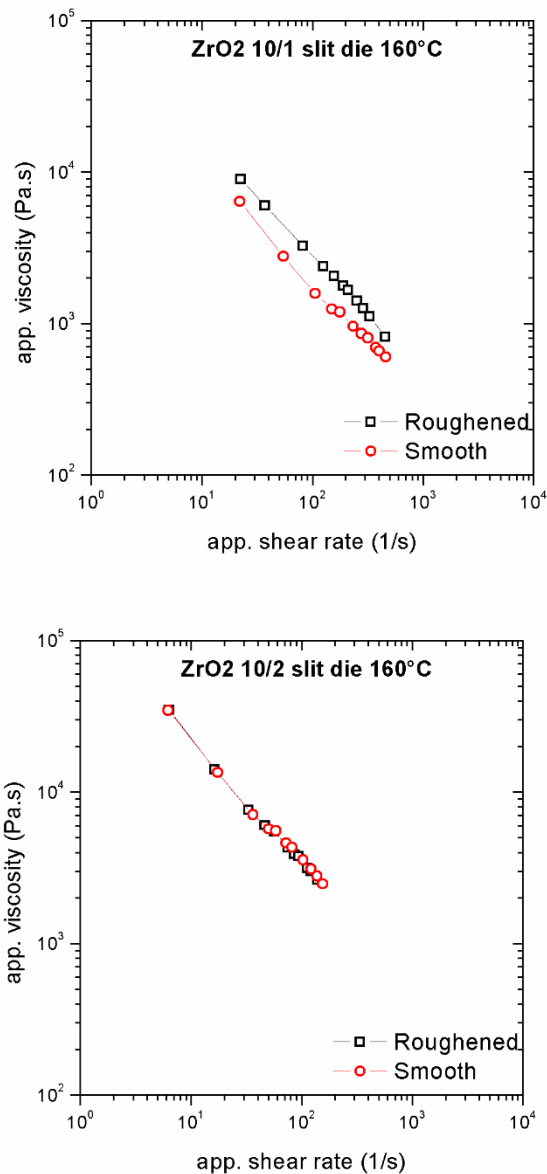


*Fig. 17 – App. viscosity as the function of app. shear rate for zirconia oxide compound extruded through smooth and roughened slit die with parameters (10/1/100) mm and (10/2/100) mm. The used temperature (related on die section) was 160°C. Differences between surface roughnesses for individual gaps.*



Fig. 17. depicted a comparison of individual gaps varies with surface properties. The flow curve, when the gap is 1 mm, is influenced by the surface roughness of the flow channel. The values for the smooth channel are below the value for the roughened channel. On the other hand, the flow curve when the gap is 2 mm is not influenced by the surface roughness.

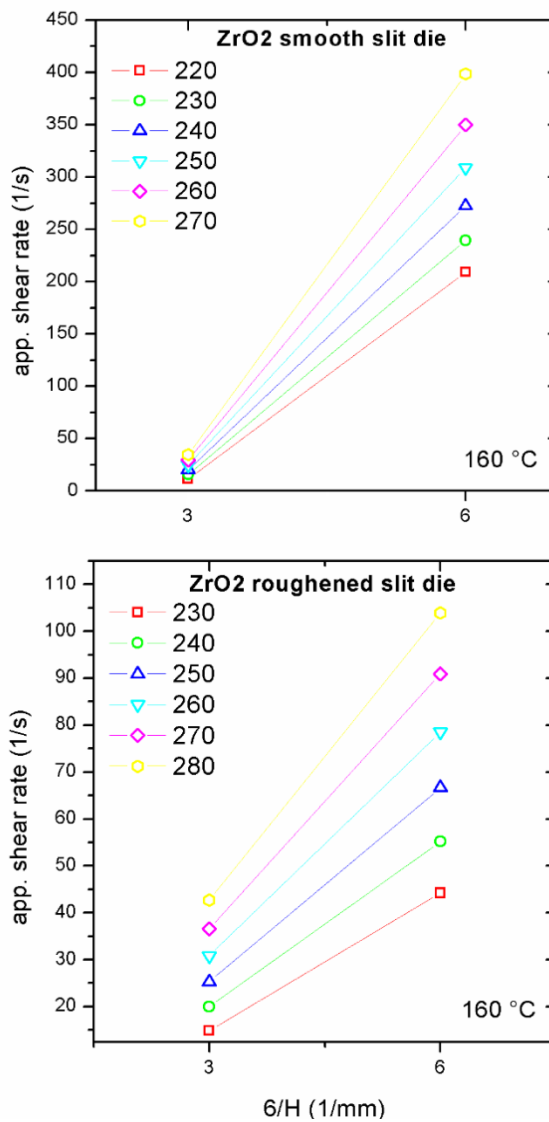
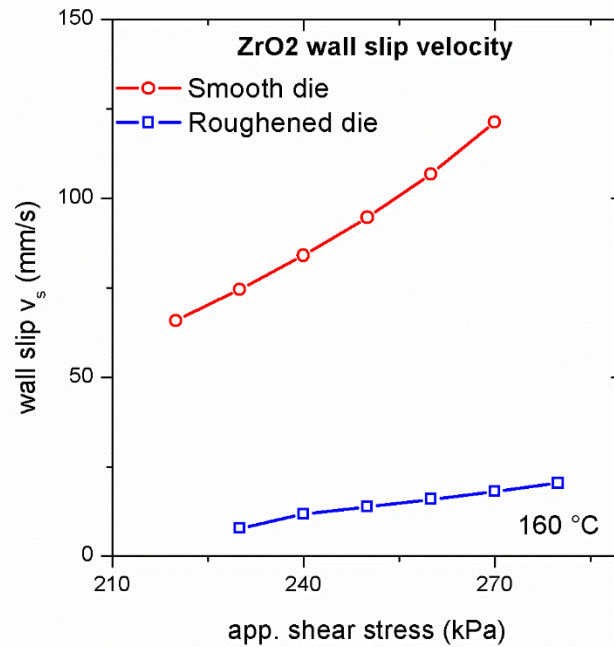


Figure 18 - Mooney plot for five values of constant wall shear stress investigated for smooth and roughened die. Linear fit is approximate but the intercept with the shear rate axis is positive for all values of shear stress.

Construction of Mooney plots was done as Fig. 18. depicted and the slope of the curves represents slip velocity.



*Figure 19 - Slip velocity as a function of wall shear stress evaluated for smooth and roughness die.*

Surface roughness effect of flow channel is really strong presented in Fig. 19. When it is compared two values of slip velocity in one value of app. shear rate, it was found out the value of slip velocity in flow channel geometry (10/1/100) mm is more than five times bigger then value flow channel geometry (10/2/100).

The second feedstock, aluminum oxide compound, was processed at same three temperature setting as before. First setting was: 130 °C, 135 °C, 140 °C, 140 °C, next one was 130 °C, 140 °C, 150 °C, 150 °C, and the last setting: 135 °C, 145 °C, 160 °C, 160 °C. The first three temperatures were set for the extrusion screw, and the last two corresponds to zones at the slit die. The flow curves for (10/1/100) mm and (10/2/100) mm slit were evaluated from the measured data and were evaluated only for setting 135 °C, 145 °C, 160 °C, 160 °C because of comparison with zirconium oxide compound. As it can be seen, surface roughness of flow channel unambiguously affects rheological behavior. First die which was tested on rheological behavior during process had a smooth surface and dimensions were (10/1/100) mm and (10/2/100) mm. In dies with smooth surface, smaller pressure gradient was expected than with the rough surface; therefore, sensors with smaller limit could be used. The first sensor  $p_1$  was situated in the end of die and had magnitude 0 – 100 bar, in the middle was sensor  $p_2$  with magnitude 0 – 350 bar and on the start was the sensor  $p_3$  with magnitude 0 – 500 bar. It was expected that pressure variation will be bigger at lower temperatures. Second die had a roughened surface and geometry shape was the same like below. There have been selected pressure sensors valve with bigger range because of roughness surface, but there was a problem during roughened channel measurement with geometry (10/2/100) mm. With a gradual increase in screw rotation speed to 30 rpm, a pressure gradient was observed which was directly proportional to the speed of rotation of the screw. At speeds over 30 rpm, however, the pressure increased to a fluctuating value and remained there until the end of the measurement. For this reason, values for roughened channel with geometry (10/2/100) mm were not calculated and we could not compare the flow behavior to (10/1/100) mm geometry and (10/2/100) mm geometry of smooth channel.

Fig. 19. Depicted dependence of the viscosity of the alumina compound on the flow channel geometry. This dependence is similar to zirconium oxide compound. This situation could be expected because the polymer matrix is the same for both compounds.

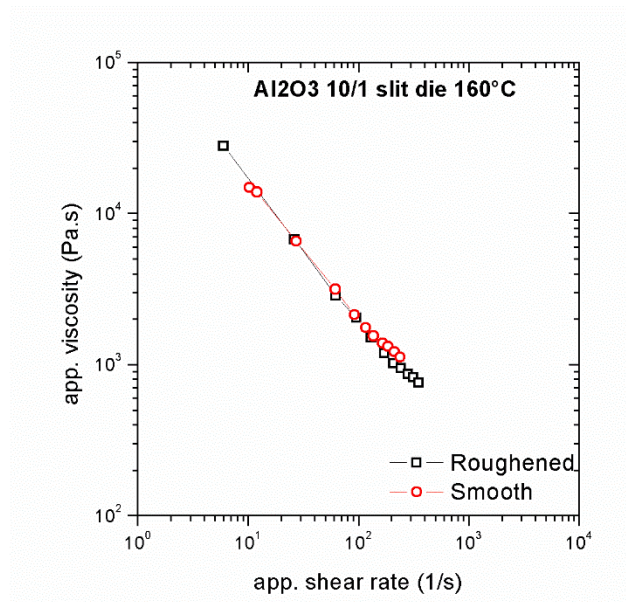


Figure 20 - App. viscosity as the function of app. shear rate for alumina oxide compound extruded through smooth and roughened slit die with parameters (10/1/100) mm. The used temperature (related on die section) was 160°C. Differences between gaps in individual roughness.

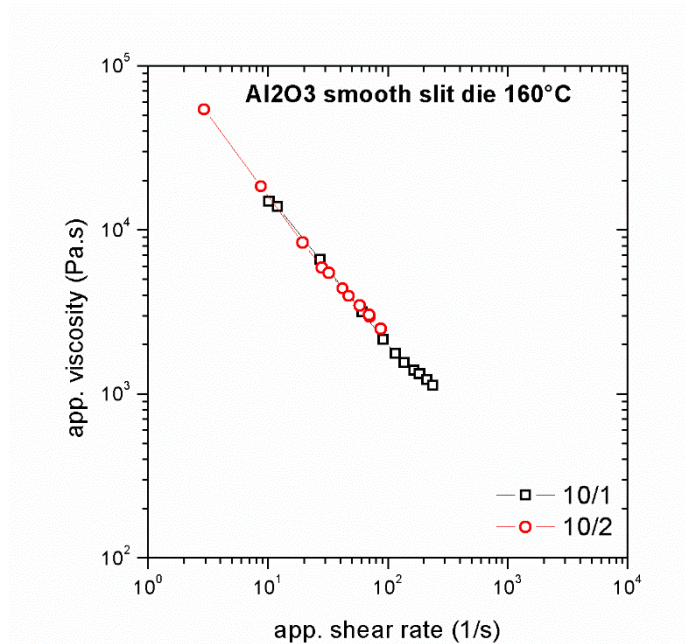


Figure 21 - App. viscosity as the function of app. shear rate for alumina oxide compound extruded through smooth slit die with parameters (10/1/100) mm and (10/2/100). The used temperature (related on die section) was 160°C. Differences between roughnesses in individual gaps.

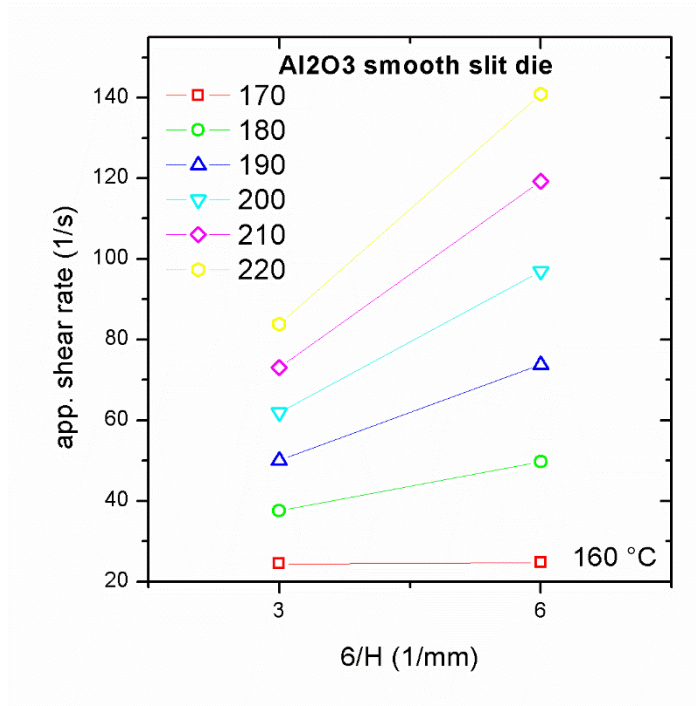


Figure 22 - Mooney plot for two values of constant wall shear stress investigated for smooth surface of flow channel. Linear fit is approximate but the intercept with the shear rate axis is positive for all values of shear stress.

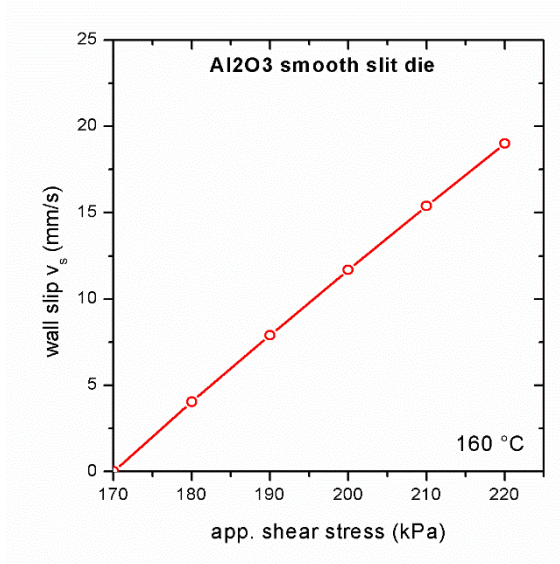
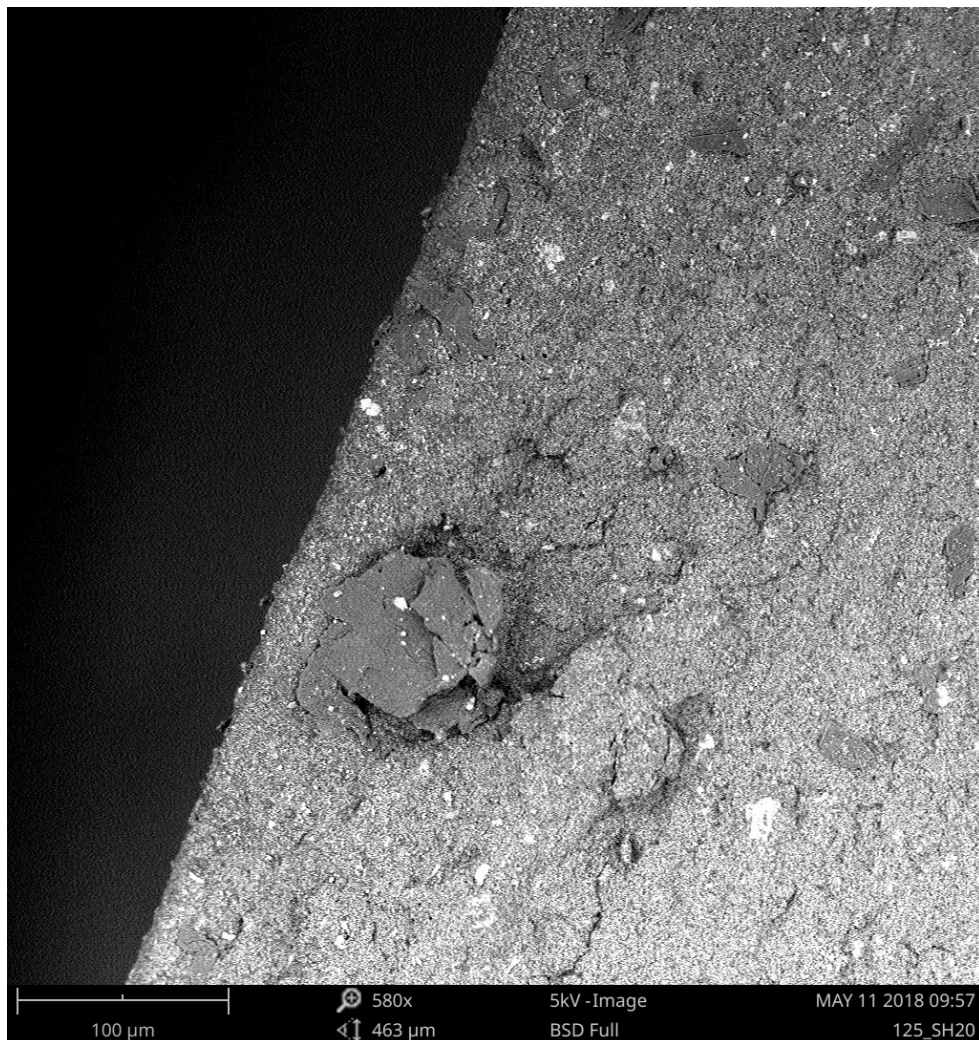


Figure 23 - Slip velocity as a function of wall shear stress evaluated for smooth die.

The calculated slip velocity for smooth die of aluminum oxide compound was not similar to the results we previously calculated for zirconium oxide compound. The result of this could be found in the particle size of the aluminum oxide. It has much smaller particles than zirconium oxide, so the surface area of the particles is much larger. This phenomenon could result in a better distribution of the polymer matrix throughout the bulk of the material and the subsequent thin layer formation. This would result in less sliding and therefore lower slip velocity.



*Figure 24 – Agglomerated powder as a result of separation for roughened geometry (10/2/100) for aluminum oxide compound.*

*Extrusion speed is 80 rpm.*

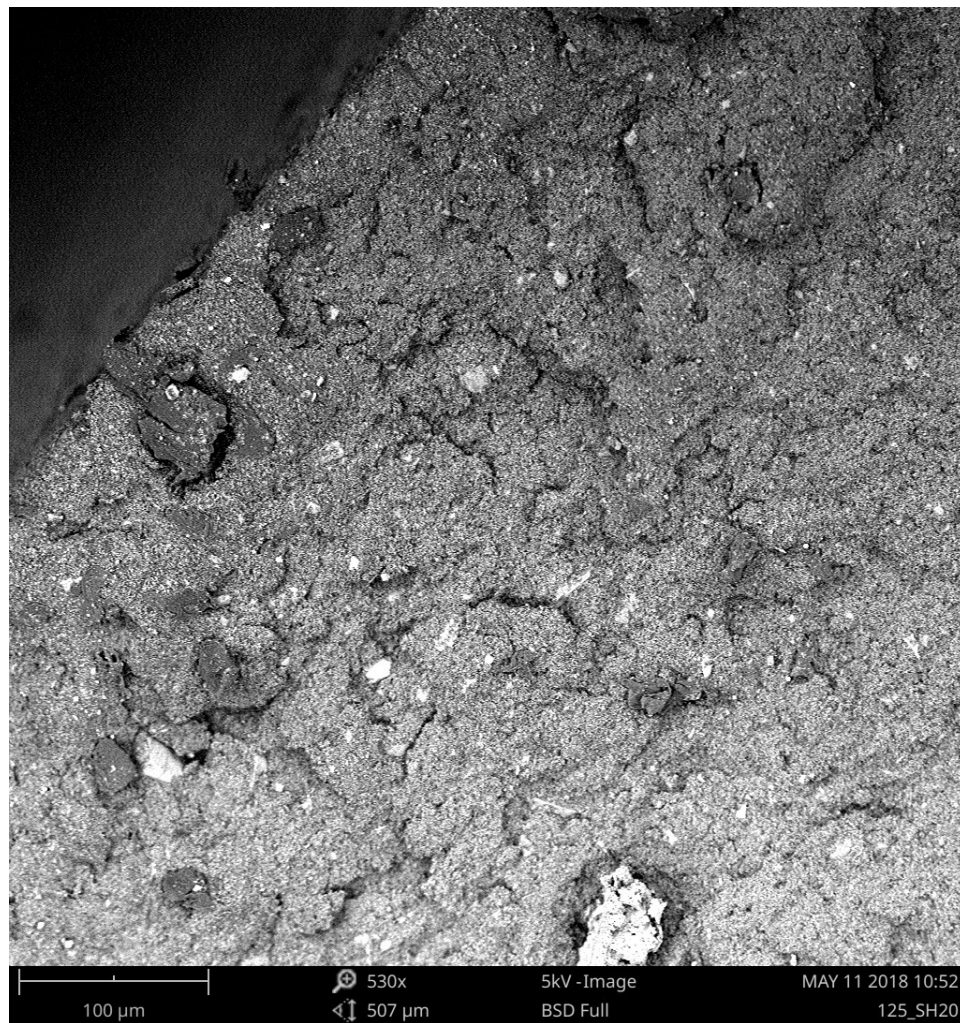


*Figure 25 - Agglomerated powder as a result of separation for roughened geometry (10/2/100) for aluminum oxide compound.*

*Extrusion speed is 100 rpm.*

Separated agglomerations, which Fig. 24. and Fig. 25 depicted, are main reason of fluctuate pressure gradient during the high speed extrusion. On the other hand, Fig. 26. depicted system without agglomerations during the low speed extrusion.

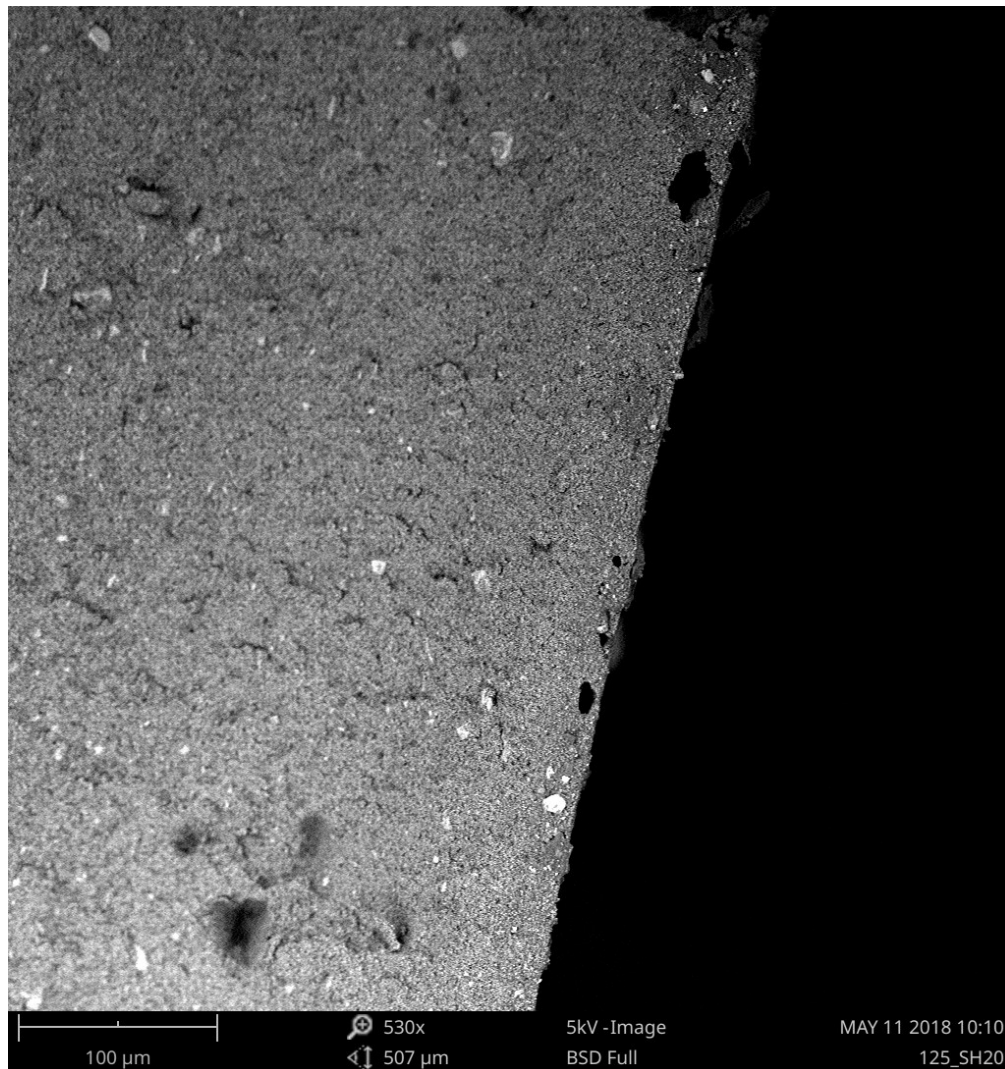


*Figure 26 – No agglomerations in roughened geometry (10/2/100) for aluminum oxide compound. Extrusion speed is 20 rpm.*



## CONCLUSION

In this master thesis the rheological properties of highly filled polymer compound of zirconium oxide and aluminum oxide were measured by means of slit die type rheometer at screw speeds typical for extrusion process. All investigated PIM feedstocks proved the pseudoplastic behavior during the flow process. At the beginning, the wall slip behavior - during the flow of zirconia oxide compound was determined with the using of on-line rheometer Brabender Extrusiograph 19/25D. The influence of slit die geometry on rheological properties was investigated in broad range of shear rates. The evaluated values of apparent shear stress and apparent shear rate were higher by using bigger gap of flow channel (10/2/100) mm than by using smaller gap (10/1/100) mm. Monitoring the rheological behavior of zirconia oxide and polymeric matrix during the process on (10/2/100) mm slit die was not possible with the batch of processing scale of temperature 135°C, 145°C, 160°C, 160°C because exceeding maximum pressure value of the transducer (700 bar). Also, the flow curves of aluminum oxide for slit die geometry (10/2/100) could not be derived because the material presented fluctuating pressure gradient during increasing screw speed. A pressure gradient was visible during the low speed rotation of the screw. After exceeding the speed of 30 rpm the pressure rised to a constant value and fluctulated. Explanation of this problem can be found in the phase separation of the suspension. During flowing in a rough die with a size of 2 mm, the solid particles were separated from the polymer matrix on the roughened surface of channel. Subsequently, the rigid particles were critically seated between micro gaps of roughened surface. Result of this phenomom is reduction in the viscosity of the material and reduction pressure in the bulk volume. Subsequent release of the unsaturated particulate layer into bulk system increases viscosity, thereby increasing the pressure in the bulk suspension volume. Beside the influence of the gap of flow channel on the rheological behavior the consequence of surface roughness of the flow channel was investigated. Dependence of the flow behavior on roughness channel was described in the case of zirconium oxide compound for all measurement. In the contrast, 2 mm gap exhibited no changes in flow curves by using the roughened flow channel. After changing to 1 mm gap differences was monitored. Dependence of the gap high presented the Mooney plot. Effect of the surface roughness is significant. Values of the shear rates by using (10/1/100) mm geometry are much bigger by using the smooth flow channel. On the other side, by using of roughness channel and the same geometry the values was significantly

smaller. This investigation rely on with following evaluations of slip velocity. Smooth channel exhibited much higher slip velocity values, than we could find in roughness channel.

**BIBLIOGRAPHY**

- [1] MARGARITA, Rueda, Martha, AUSCHER, Marie-Camille, FULCHIRON René, PÉRIÉ, Thomas, MARTIN, Grégory, SONNTAG, Philippe, CASSAGNAU, Philippe. Rheology and applications of highly filled polymers: A review of current understanding. *Progress in Polymer Science*, 20017, 66, 22–53. ISSN: 0079-6700
- [2] KALYON, D. M., YILMAZER, U. (Rheological behaviour of highly filled suspensions which exhibit slip at the wall. *Highly Filled Material Institute*, 1990, 241-273.
- [3] BARNES, H. A. A review of the slip (wall depletion) of polymer solutions, emulsions and particle suspensions in viscometechologyers: its cause, character, and cure. *Journal of Non-Newtonian Fluid Mechanics*, 1995, 56(3), 221-251
- [4] GADELMAWLA, E.S., KOURA M.M., MAKSOU, T.M.A. ELEWA, I.M., SOLIMAN, H.H. Roughness parameters, *Journal of Material Processing Technology*, 2002, 123, 133-145. ISSN: 0924-0136.
- [5] BAUZAA, M.B., WOODYA, S.C., WOODYA, B.A., SMITH, S.T. Surface profilometry of high aspect ratio features. *Wear*, 2011, 271, 519–522. ISSN: 0043-1648
- [6] ZHONG, Min, CHEN, Feng, XIAO, Chao, WEI, Yongchao. 3-D surface profilometry based on modulation measurement by applying wavelet transform method. *Optics and Lasers in Engineering*, 2016, 88, 243–254. ISSN: 0143-8166
- [7] DE GROOT P. Coherence Scanning Interferometry, *Optical Measurement of Surface Topography*, 2011. ISBN:978-3-642-12012-1.
- [8] FAY, Martin, F., DE LEGA, Xavier, Colonna, DE GROOT, Peter. Measuring High-Slope and Super-Smooth Optics with High-Dynamic-Range Coherence Scanning Interferometry, *Zygo Corporation, Laurel Brook Lane*. 2014.

- [9] STOUT, J , S., SULLIVAN, J., DONG, W.,MAINSAH, E, LUO, N. *The Development of Methods for the Characterization of Roughness in Three Dimension*, The University of Birmingham U. K. ISBN: 0 7044 1313 2
- [10] SAKETI , S., ÖSTBY , J., OLSSON , M. Influence of tool surface topography on the material transfer tendency and tool wear in the turning of 316L stainless steel, *Wear*, 2016, 368-369, 239–252. ISSN: 0043-1648
- [11] GULMUS, Sergul Acikalin, YILMAZER, Ulku. Effect of the Surface Roughness and Construction Material on Wall Slip in the Flow of Concentrated Suspensions. *Journal of Applied Polymer Science*, 2006, 103, 3341–3347.
- [12] SHIVASHANKAR T. S., ENNETI R. S., PARK S. J., GERMAN R. M., ATRE S. V., The effects of material attributes on powder-binder separation phenomena in powder injection molding, *Powder Technology*, 2013, 243, 79-84. ISSN: 0032-5910
- [13] ACRIVOS, A., MAURI, R.,FAN, X. Shear-induced resuspension in a couette device, *International Journal of Multiphase Flow*, 1993, 19(3), 797-802, ISSN: 0301-9322
- [14] ALLENDE M., FAIR D., KAYLON D.M., CHIU D., MOY S. Development of Particle Concentration Distribution and Burning Rate Gradients upon Shear Induced Particle, Migration during Processing of Energetic Suspensions, *Journal of Energy Mater*, 2007, 25(1), 49-67.
- [15] YILMAZER, U., KALYON, D. M. Slip effects in capillary and parallel disk torsional flows of highly filled suspensions. *Journal of Reology*, 1989, 33, 8. ISSN 0148-6055
- [16] VAND, V. Viscosity of solutions and suspensions, *Journal of Physical and Colloid Chemistry*, 1948, 52, 277.

- [17] BINGHAM, Eugene. Fluidity And Plasticity, New york: Mcgraw-Hill Book Company,Inc.
- [18] KALYON, Dilhan, M. Apparent slip and viscoplasticity of concentrated suspensions. *The Society of Rheology*, 2005, 49(3), 621-640.
- [19] MAZZANTI, Valentina, MOLLICA, Francesco. Pressure dependent wall slip of wood flour filled polymer melts. *Journal of Non-Newtonian Fluid Mechanics*, 2017, 247, 178–187. ISSN: 0377-0257
- [20] YILMAZER, U. GOGOS, C. G., KALYON, D. M. . Mat formation and unstable flows of highly filled suspensions in capillaries and continuous processors. *Polymer Composites*, 1989, 10, 4, 242-249. ISSN 0272-8397
- [21] HATZIKIRIAKOS, Savvas, G. Wall slip of molten polymers, *Progress in Polymer Science*, 2012, 37, 624– 643. ISSN: 0079-6700
- [22] YOSHIMURA, A. S., PRUDHOMME, R. K, Wall Slip Corrections For Couette And Parallel Disk Viscometers, *Journal of Rheology* , 1988, 32, 53, ISSN: 0148-6055
- [23] SUPATI, R., LOH, KHOR, N.H., K.A., TOR , S.B. Mixing and characterization of feedstock for powder injection molding, *Materials Letters*, 2000, 4, 109–114. ISSN: 0167-577X
- [24] STEFFE, J. F. Rheological methods in food process engineering, second ed. *Freeman Press*, 1996, 418.
- [25] HAN, Chang. *Entrance region flow of polymer melts*, American Institute of Chemical Engineers, 1971, 17(6). ISSN:1547-5905

**LIST OF ABBREVIATIONS**

2D	Two dimension
3D	Three dimension
SEM	Scanning electron microscope
SPM	Scanning probe microscope
Å	Ångström
CSI	Coherence scanning interferometry
DNR	Dynamic noise reduction
HDR	High dynamic range
$R_a$	Arithmetic average high
$R_y$	Maximum depth valley
$R_{max}$	Maximum high of profile
$R$	Radius
$H$	Flow channel gap
$\delta$	Slip layer thickness
KCl	Potassium chloride
EDX	Energy disperse X-Ray
LDPE	Low-density polyethylene
EVA	Ethylene-vinyl acetate
PIM	Powder injection molding
°C	Degree Celsius
CIM	Ceramic injection molding
$W$	Width
$L$	Length
$S_a$	Arithmetic mean deviation of the surface

$Al_2O_3$  Alumina oxide

$ZrO_2$  Zirconium oxide

## LIST OF FIGURES

<i>Figure 1 - Definition of the arithmetic average height. [4]</i> .....	15
<i>Figure 2 - Definitions of the parameters <math>R_v</math>, <math>R_p</math>, <math>R_t</math> (<math>R_{max.}</math>). [4]</i> .....	16
<i>Figure 3 – Demonstrating of one example evaluation. In actuality, all surface height changes are evaluated[11]</i> .....	17
<i>Figure 4 - Differences between no-slip (left) situation and true slip (right). [13]</i> .....	18
<i>Figure 5 - Differences between no-slip(left) situation and apparent slip(right).[13]</i>	20
<i>Figure 6 - Wall shear stress vs. apparent shear rate for four slit dies. [20]</i> .....	20
<i>Figure 7 - Representation of shear stress and velocity profile in capillary flow with apparent wall slip .[21]</i> .....	21
<i>Figure 8 - Schematic representation of the apparent slip flow: (a) in plane Couette (pure drag) flow; (b) in capillary (radius, R).[19]</i> .....	22
<i>Figure 9 - Velocity profiles in simple shear (plane Couette flow) under no-slip (left) and slip conditions (right).[19]</i> .....	23
<i>Figure 10 - The formation of the apparent slip layer upon the capillary flow of a concentrated suspension of particles incorporated into an elastomeric binder.[19]</i> .....	23
<i>Figure 11 - Schematic diagram for the effect of <math>R_a</math> size ratio on the wall slip velocity.[3]</i> .....	26
<i>Figure 12 - Particles size distribution of aluminum oxide. ....</i>	29
<i>Figure 13 - Setting of three locations of measuring. ....</i>	31
<i>Figure 14 - The last output of ZYGO software with evaluated parameters and graphically presented surface. ....</i>	32
<i>Figure 15 - Scheme of measuring device with representation of pressure (<math>p_1 - p_3</math>).33</i>	33
<i>Figure 16 – App. viscosity as the function of app. shear rate for zirconia oxide compound extruded through smooth and roughened slit die with parameters (10/1/100) mm and (10/2/100) mm. The used temperature (related on die section) was 160°C. Differences between gaps in individual surface roughness.....</i>	38
<i>Fig. 17 – App. viscosity as the function of app. shear rate for zirconia oxide compound extruded through smooth and roughened slit die with parameters (10/1/100) mm and (10/2/100) mm. The used temperature (related on die section) was 160°C. Differences between surface roughnesses for individual gaps. ....</i>	39



- Figure 18 - Mooney plot for five values of constant wall shear stress investigated for smooth and roughened die. Linear fit is approximate but the intercept with the shear rate axis is positive for all values of shear stress. ....40*
- Figure 19 - Slip velocity as a function of wall shear stress evaluated for smooth and roughness die. ....41*
- Figure 20 - App. viscosity as the function of app. shear rate for alumina oxide compound extruded through smooth and roughened slit die with parameters (10/1/100) mm. The used temperature (related on die section) was 160°C. Differences between gaps in individual roughness. ....43*
- Figure 21 - App. viscosity as the function of app. shear rate for alumina oxide compound extruded through smooth slit die with parameters (10/1/100) mm and (10/2/100). The used temperature (related on die section) was 160°C. Differences between roughnesses in individual gaps. ....43*
- Figure 22 - Mooney plot for two values of constant wall shear stress investigated for smooth surface of flow channel. Linear fit is approximate but the intercept with the shear rate axis is positive for all values of shear stress. ....44*
- Figure 23 - Slip velocity as a function of wall shear stress evaluated for smooth die. ....44*
- Figure 24 – Agglomerated powder as a result of separation for roughened geometry (10/2/100) for aluminum oxide compound. Extrusion speed is 80 rpm. ....45*
- Figure 25 - Agglomerated powder as a result of separation for roughened geometry (10/2/100) for aluminum oxide compound. Extrusion speed is 100 rpm. ....46*
- Figure 26 – No agglomerations in roughened geometry (10/2/100) for aluminum oxide compound. Extrusion speed is 20 rpm. ....47*

**LISTO OF TABLE**

<i>Table 1 – Characteristic of the binder. ....</i>	<i>28</i>
<i>Table 2 - Characteristic of aluminum oxide powder. ....</i>	<i>28</i>
<i>Table 3 - Characteristic of powder ZrO<sub>2</sub>. ....</i>	<i>29</i>
<i>Table 4 - The roughness parameters of smooth and roughened slit die flow channels. ....</i>	<i>35</i>